On the Mechanism of Re(I)−Carboxylate Bond Cleavage by Perchloric Acid: A Kinetic and Spectroscopic Study

ARTICLE *in* THE JOURNAL OF PHYSICAL CHEMISTRY A · AUGUST 2011

Impact Factor: 2.69 · DOI: 10.1021/jp206328q · Source: PubMed

THE JOURNAL OF PHYSICAL CHEMISTRY A

ARTICLE

pubs.acs.org/JPCA

On the Mechanism of Re(I)−Carboxylate Bond Cleavage by Perchloric Acid: A Kinetic and Spectroscopic Study

Ulises N. Fagioli, Fernando S. García Einschlag, Carlos J. Cobos, Gustavo T. Ruiz, Mario R. Féliz, and Ezequiel Wolcan*

Instituto de Investigaciones Fisicoquímicas Teóricas y Aplicadas (INIFTA), Departamento de Química, Facultad de Ciencias Exactas, Universidad Nacional de La Plata, Casilla de Correo 16, Sucursal 4, (1900) La Plata, Argentina

ABSTRACT: We have studied the reaction between pz−CO_2−Re(CO)$_3$(bpy) and perchloric acid in acetonitrile by following the UV−vis and IR spectral changes in the reaction mixture. A fast equilibrium was found to be established between solvated protons, pz−CO_2−Re(CO)$_3$(bpy), and the protonated intermediate [pz−C(OH)O−Re(CO)$_3$(bpy)]$^+$ which finally yields pz−COOH and Re(CO)$_3$(bpy)(CH$_3$CN)$^+$ as reaction products. This intermediate has been characterized by UV−vis and IR spectroscopies and by DFT calculations. The fully optimized DFT/CPCM structures for pz−CO_2−Re(CO)$_3$(bpy) and [pz−C(OH)O−Re(CO)$_3$(bpy)]$^+$ were compared with the X-ray structure of pz−CO_2−Re(CO)$_3$(bpy). The structural parameters associated with the carboxyl group in the protonated intermediate are between those of pz−CO_2−Re(CO)$_3$(bpy) and pz−COOH. Multivariate curve resolution methods were employed to obtain the spectrum of the protonated intermediate and the concentration profiles from the full matrix of time-resolved UV−vis spectra. The proposed mechanism was numerically simulated by using Runge−Kutta methods. Model parameters were estimated by nonlinear regression fitting of the concentration profiles, yielding values of $\log(K) = 4.9 \pm 0.3$ and $k = 0.16 \pm 0.03$ min^{-1} for the formation equilibrium constant and the decay rate constant of the protonated intermediate, respectively.

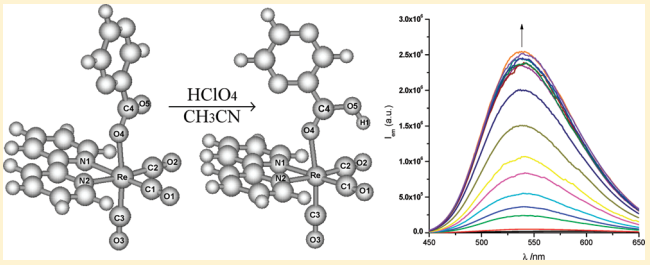

INTRODUCTION

Among the third row of transition metal compounds, Re(I) tricarbonyl complexes coordinated to mono- or bidentate azines of the type *fac*-XRe(CO)$_3$L (where X = halide and/or substituted azine and L= α-diimine) show exceptionally rich excited-state behavior and redox chemistry as well as thermal and photochemical stability.[1,2] The substitution of the halide ligand X by a spectator ligand (L_S) has provided useful procedures for the preparation of related *fac*-L_SRe(CO)$_3$L complexes that might be utilized in electron transfer studies,[3] solar energy conversion,[4−6] and catalysis.[7,8] Possible applications as luminescent sensors[9−11] and molecular materials for nonlinear optics[12,13] or optical switching[14] have also emerged. In particular, luminescent transition metal complexes of Re(I) and Ru(II) with polypyridil ligands have been recognized as good potential candidates for the development of pH-sensing devices.[15] We have previously studied the photophysical and photochemical properties of a series of *fac*-L_S−CO_2−Re(CO)$_3$L complexes (with L_S = 2-pyrazine, 2-naphthalene, 9-anthracene, 1-pyrene, acetate, 2-anthraquinone, ferrocene and L = 2,2′-bipyridine and/or 1,10-phenanthroline) where the spectator ligand is bridged by a carboxylate group.[16−20] In this paper, we study the solvolysis of pz−CO_2−Re(CO)$_3$(bpy) (pz = 2-pyrazine, bpy = 2,2′-bipyridine) induced by perchloric acid in acetonitrile solutions, eq 1:

$$\text{pz}-\text{CO}_2 - \textit{Re}(\text{CO})_3(\text{bpy}) \xrightarrow[\text{CH}_3\text{CN}]{\text{HClO}_4} [\text{Re}(\text{CO})_3(\text{bpy})(\text{CH}_3\text{CN})^+] + \text{ClO}_4^- + \text{pz}-\text{COOH} \quad (1)$$

The kinetics of the reaction was studied by UV−vis and FTIR spectroscopies. A protonated intermediate, [pz−C(OH)−O−Re(CO)$_3$(bpy)]$^+$, was characterized by UV−vis/IR spectroscopy and by DFT calculations. A fast equilibrium was found to be established between solvated protons, pz−CO_2−Re(CO)$_3$(bpy), and the protonated intermediate [pz−C(OH)O−Re(CO)$_3$(bpy)]$^+$, which finally yields pz−COOH and Re(CO)$_3$(bpy)(CH$_3$CN)$^+$ as reaction products. After the termination of the reaction, a great enhancement of the luminescence is observed due to the fact that the product [Re(CO)$_3$(bpy)(CH$_3$CN)$^+$] is a much stronger luminophore than the parent complex pz−CO_2−Re(CO)$_3$(bpy). Moreover, the process described by eq 1 could be utilized for the development of a device capable of detecting proton traces in aprotic media as well as in a pH-sensing material.

EXPERIMENTAL SECTION

Materials. The complexes pz−CO_2−Re(CO)$_3$(bpy) and CF_3SO_3Re(CO)$_3$(bpy) were available from previous work.[16,21] Given that in acetonitrile solutions $CF_3SO_3^-$ is replaced by the solvent, the solvated species will be denoted as [Re(CO)$_3$(bpy)(CH$_3$CN)$^+$]. All other chemicals, commercially available products

Received: July 5, 2011
Revised: August 30, 2011
Published: August 30, 2011

of highest possible quality (Aldrich, Fluka, Riedel de Haën, Baker), were used without further purification.

General Methods. UV−vis spectra were recorded on a Shimadzu UV-1800 spectrophotometer. FTIR spectra were recorded on a Nicolet 8700 Thermo Scientific.

Photophysical Measurements. Emission spectra were obtained with a computer-interfaced near-IR Fluorolog-3 research spectrofluorometer. Spectra were corrected for differences in spectral response and light scattering. Solutions were deaereated with O_2-free nitrogen in a gas-tight apparatus before recording the spectra.

Emission quantum yields, ϕ_{em}, were measured relative to Rhodamine B in ethanol ($\phi_{ref} = 0.69$). Quantum yields were calculated according to the equation

$$\phi_{em} = \left(\frac{A_{ref}}{A_s}\right)\left(\frac{I_s}{I_{ref}}\right)\left(\frac{n_s}{n_{ref}}\right)^2 \phi_{ref} \quad (2)$$

where I_s and I_{ref} represent the integral of the emission spectrum for the sample and the reference, whereas A_s and A_{ref} stand for the absorbances of the sample or reference at the excitation wavelength ($A_{\lambda exc} < 0.1$) and n is the solvent refraction index. The excitation wavelength used was $\lambda_{exc} = 375$ nm.

Spectroscopic Analysis. For the analysis of the time-resolved spectra, we used a software designed in our laboratory[22] capable to perform "multivariate curve resolution" (MCR).[23,24] These methods can be applied to bilinear spectroscopic-kinetic data from a chemical reaction to provide information about composition changes in an evolving system.[25] In the present work we have chosen one of the most widely used algorithms, the alternating least-squares (ALS), which can help to estimate concentration and spectral profiles simultaneously.[25,26] The ALS algorithm extracts useful information from the experimental data matrix $\mathbf{A}(t \times w)$ by iterative application of regression analysis using the following matrix product

$$\mathbf{A} = \mathbf{C}\mathbf{S}^T + \mathbf{E} \quad (3)$$

where $\mathbf{C}(t \times n)$ is the matrix of the kinetic profiles, $\mathbf{S}^T(n \times w)$ is that containing the spectral profiles, and $\mathbf{E}(t \times w)$ represents the error matrix. The numbers t, n, and w denote the sampling times, absorbing species, and recorded wavelengths, respectively. Resolving matrix $\mathbf{A}$ may be a rather difficult task[27] since on the one hand n is usually unknown,[28] and on the other hand curve resolution methods cannot deliver a single solution because of rotational and scale ambiguities.[29] We applied factor analysis and singular value decomposition to the experimental matrix for the estimation of n. In order to reduce rotational ambiguities, we used some chemically relevant constraints[30] such as non-negativity, selectivity, and unimodality. Matrix augmentation strategy was used to simultaneously obtain the concentration profiles corresponding to different experimental conditions.[26]

Kinetic Analysis. The system of coupled differential equations that describes the proposed mechanism was numerically simulated by using the fourth-order Runge−Kutta method.[31] Model parameters were estimated by nonlinear regression fitting of the rate constants to the concentration profiles. Nonlinear regression was performed by using the steepest descendent method.[32] For kinetic analysis we have used the software mentioned above.[22]

Computational Details. Quantum mechanical calculations can be very helpful to explain physicochemical properties of Re(I) complexes.[33] In fact, density functional theory (DFT) and time-dependent density functional theory (TD-DFT) calculations of ground- and excited-state properties of a series of Re(I) tricarbonyl complexes have been recently employed to interpret the experimental absorption bands arising from a set of metal-to-ligand charge transfer transitions (MLCT), ligand-to-ligand charge transfer transitions (LLCT), and intraligand transitions (IL).[33,34] In the present work, the B98 hybrid funtional[35] has been employed to optimize via analytic gradient methods the structure of the pz−CO_2−Re(CO)$_3$(bpy) and [pz−C(OH)O−Re(CO)$_3$(bpy)]$^+$ species as implemented in the Gaussian 09 program package.[36] In the absence of the traditional Pople's[37] or Dunning's correlation consistent basis sets[38] for the Re atom, the effective core potential basis set LanL2DZ[39] was employed for all atoms. However, no significant differences were observed by replacing the LanL2DZ basis set by the Pople's 6-311++G(d,p) basis set for the H, C, N, and O atoms. Bulk solvent effects were accounted for employing the conductor-like polarizable continuum model, CPCM,[40] with a dielectric constant for acetonitrile of 35.688. For both studied molecules, positive vibrational frequencies were obtained assuring that computed molecular structures are stable. A proton was added to the O atom not bonded to the Re atom in the pz−CO_2−Re(CO)$_3$(bpy) molecule as the starting point for the optimization of the intermediate structure.

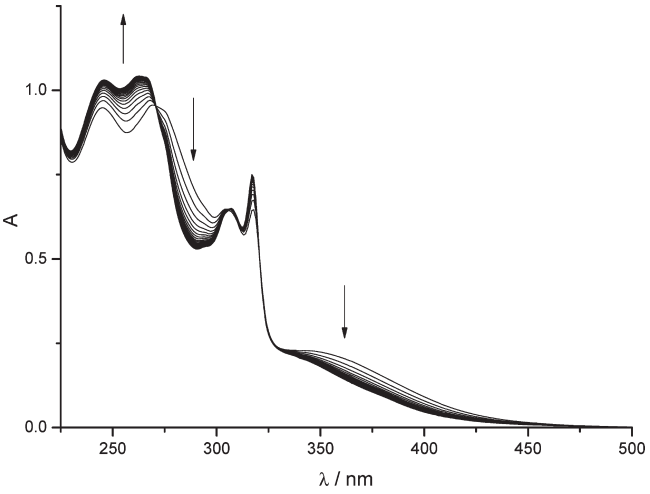

Figure 1. Typical spectral changes following the mixing of pz−CO_2−Re(CO)$_3$(bpy) and $HClO_4$ solutions with [Re(I)] = 5×10^{-5} M and [$HClO_4$] = 5×10^{-5} M in acetonitrile. The arrows show the progress of the change made every 2 min from $t = 1$ min up to 49 min. See text for details.

RESULTS AND DISCUSSION

Reaction Rate Measurements. Absorbance changes in the UV−vis spectrum were recorded at appropriate intervals following the rapid mixing of pz−CO_2−Re(CO)$_3$(bpy) and $HClO_4$ solutions in acetonitrile at room temperature (293 ± 3 K). In all the experiments, the ionic strength was fixed at 0.01 M with a solution of $(Bu_4N)PF_6$. In reaction rate measurements, the initial concentration of the Re(I) complex was kept at 5×10^{-5} M while the initial concentration of $HClO_4$ was varied from 5×10^{-6} to 1×10^{-4} M. Figure 1 shows typical spectral changes following the mixing of complex and $HClO_4$ solutions with [Re(I)] = 5×10^{-5} M and [$HClO_4$] = 5×10^{-5} M in acetonitrile. During the time course of the reaction, there is an absorbance increase in the 220−270 nm range and an

absorbance decrease in the 270−310 nm range. Besides, the lowest energy absorption band of pz−CO_2−Re(CO)$_3$(bpy), centered at λ_{max} = 365 nm, experiences a blue shift and eventually becomes a shoulder in the spectrum of the final products of the reaction.

Figure 2 shows the spectra obtained after the termination of the reaction at different [$HClO_4$]/[Re(I)] initial ratios. The inset to Figure 2 shows the consumption of the reactant and product accumulation as a function of [$HClO_4$]/[Re(I)] initial ratio obtained by applying MCR−ALS analysis to the spectra of Figure 2. The latter data are consistent with a 1:1 stoichiometry between $HClO_4$ and Re(I) complex. The UV−vis spectra of the final reaction mixture can be reproduced by summing the separate spectra of Re(CO)$_3$(bpy)(CH_3CN)$^+$ and 2-pyrazine carboxylic acid (pz−COOH), respectively (see Figure 3 below).

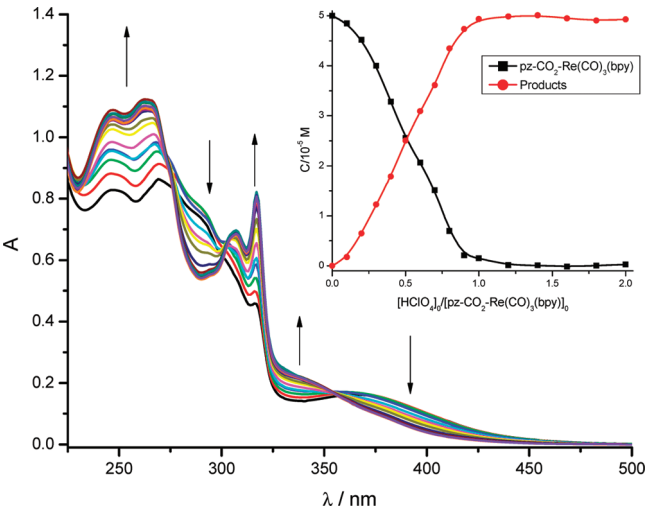

Figure 2. UV−vis spectra obtained after the termination of the reaction between pz−CO_2−Re(CO)$_3$(bpy) and $HClO_4$ at different [$HClO_4$]/[Re(I)] initial ratios. The inset to Figure 2 shows the consumption of the reactant and product accumulation as a function of [$HClO_4$]/[Re(I)] initial ratio obtained by applying MCR−ALS analysis to the spectra of Figure 2. See text for details.

Spectral changes following the mixing of pz−CO_2−Re(CO)$_3$(bpy) and $HClO_4$ solutions were recorded for [$HClO_4$]/[Re(I)] initial ratios between 0.1 and 2.0. The analysis of the full (augmented) matrix of time-resolved UV−vis spectra was performed using chemometric techniques. Both factor analysis and singular value decomposition were used for the estimation of the number of independent contributions yielding n values of 3. The orthogonal projection approach was used to obtain initial guesses of the spectra corresponding to each contributing species.[41] The spectral shapes obtained by the MCR−ALS method for the three species are those for the reactant (pz−CO_2−Re(CO)$_3$(bpy)), a protonated intermediate (hereby denoted as [pz−C(OH)O−Re(CO)$_3$(bpy)]$^+$), and the product (the sum of Re(CO)$_3$(bpy)(CH_3CN)$^+$ and pz−COOH spectra) (see Figure 3). The UV−vis spectrum of the protonated intermediate is similar to that of Figure 1 at t = 1 min after the mixing of the reactants. Moreover, the same spectral features of the protonated intermediate were observed immediately following the rapid mixing of pz−CO_2−Re(CO)$_3$(bpy) and $HClO_4$ solutions in acetonitrile (i.e., a similar spectrum to that of Figure 1 at t = 1 min was recorded at $t \sim$ 3 s.). Since, in all cases, MCR−ALS analysis showed that both pz−CO_2−Re(CO)$_3$(bpy) and [pz−C(OH)O−Re(CO)$_3$(bpy)]$^+$ species decay within the same time scale and with similar apparent rate constants, a rapid equilibrium between the reactants and the intermediate was assumed to be established just after the protonation reaction is triggered.

The nature of the reaction products was confirmed by following the IR spectral changes at appropriate time intervals after the rapid mixing of the reactants. Figure 4a shows the spectrum of pz−CO_2−Re(CO)$_3$(bpy) and the changes in the IR spectrum of the reaction mixture after the protonation of the complex followed by FTIR spectroscopy in the region of CO stretching vibrations. The parent complex displays IR spectra consistent both with the facial configuration of the carbonyl ligands and with its C_s symmetry, as witnessed by the presence of three intense absorptions which are observed in the 2025 and 1880 cm^{-1}

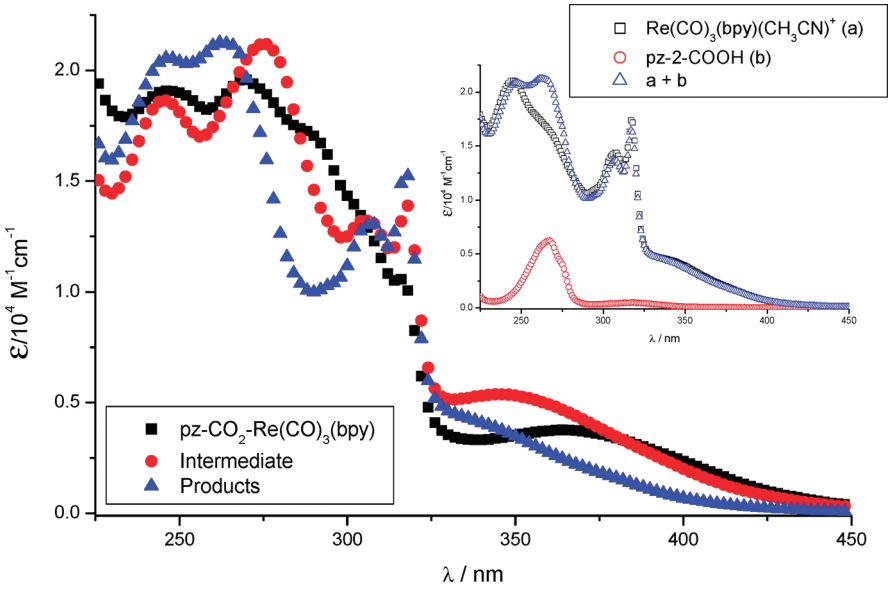

Figure 3. UV−vis spectra of pz−CO_2−Re(CO)$_3$(bpy), protonated intermediate [pz−C(OH)O−Re(CO)$_3$(bpy)]$^+$, and reaction products Re(CO)$_3$(bpy)(CH_3CN)$^+$and pz−COOH.

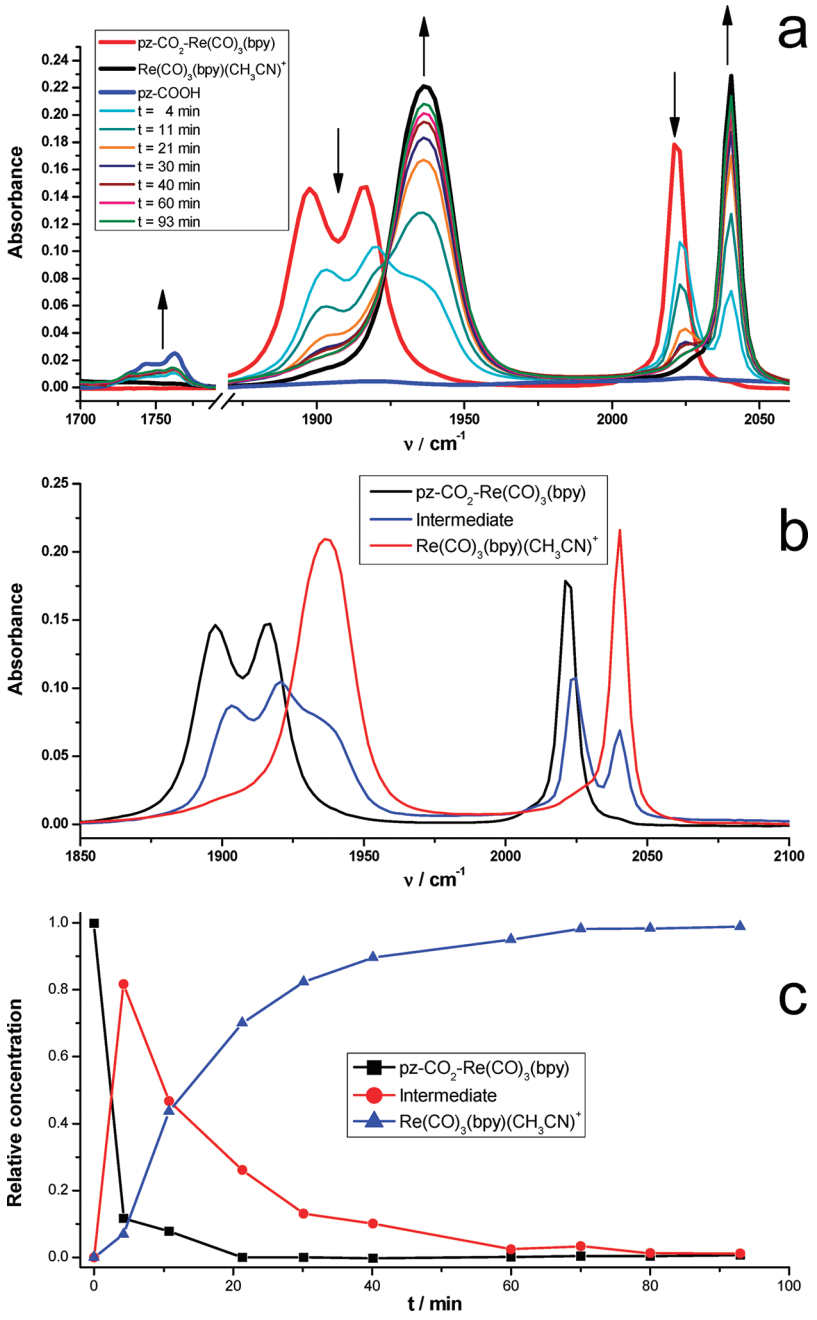

Figure 4. (a) Changes in the IR spectrum of the reaction mixture after the protonation of the complex pz−CO_2−$Re(CO)_3$(bpy) followed by FTIR spectroscopy in the region of CO-stretching vibrations with [Re(I)] = 1 × 10^{-3} M and [$HClO_4$] = 1 × 10^{-3} M in acetonitrile. Spectra of pz−CO_2−$Re(CO)_3$(bpy), $Re(CO)_3$(bpy)(CH_3CN)$^+$, and pz−COOH are included for comparative purposes. (b) Spectral shapes obtained for the three species, i.e., pz−CO_2−$Re(CO)_3$(bpy), the protonated intermediate [pz−C(OH)O−$Re(CO)_3$(bpy)]$^+$, and the reaction product $Re(CO)_3$(bpy)(CH_3CN)$^+$ from chemometric analysis of IR spectral changes. (c) Calculated concentration profiles for the three species. See text for details.

regions. According to previous reports on similar compounds, the sharp band at higher frequency, about 2023 cm^{-1}, is attributed to the A'_1 mode (totally symmetric in-phase stretching of the three CO ligands), whereas the remaining two bands at intermediate and lower frequencies (1917 and 1898 cm^{-1}) are assigned to the A'_2 (totally symmetric out-of-phase stretching) and A″ modes (asymmetric stretching of the equatorial CO ligands).[42] As can be seen in Figure 4, the CO frequencies at 1898, 1917, and 2023 cm^{-1}, belonging to pz−CO_2−$Re(CO)_3$(bpy), decrease, and the formation of a new species is evidenced by the new CO-stretching vibrations at 1936 and 2040 cm^{-1}. The spectral changes of Figure 4a can be compared with the IR spectrum of $Re(CO)_3$(bpy)(CH_3CN)$^+$, which is also shown in this figure. The IR spectrum of $Re(CO)_3$(bpy)(CH_3CN)$^+$ displays two CO-stretching vibrations at 1936 and 2040 cm^{-1}, in agreement with the CO-stretching frequencies previously reported[43] for $Re(CO)_3$(bpy)(CH_3CN)$^+$ in CH_2Cl_2 solution. As sometimes observed in *fac*-[Re(bpy)$(CO)_3$(L)]-type complexes, in the case of $Re(CO)_3$(bpy)(CH_3CN)$^+$, the A'_2 and A″ bands are superimposed into a single broad band.[43] The spectrum

dx.doi.org/10.1021/jp206328q |*J. Phys. Chem. A* 2011, 115, 10979–10987

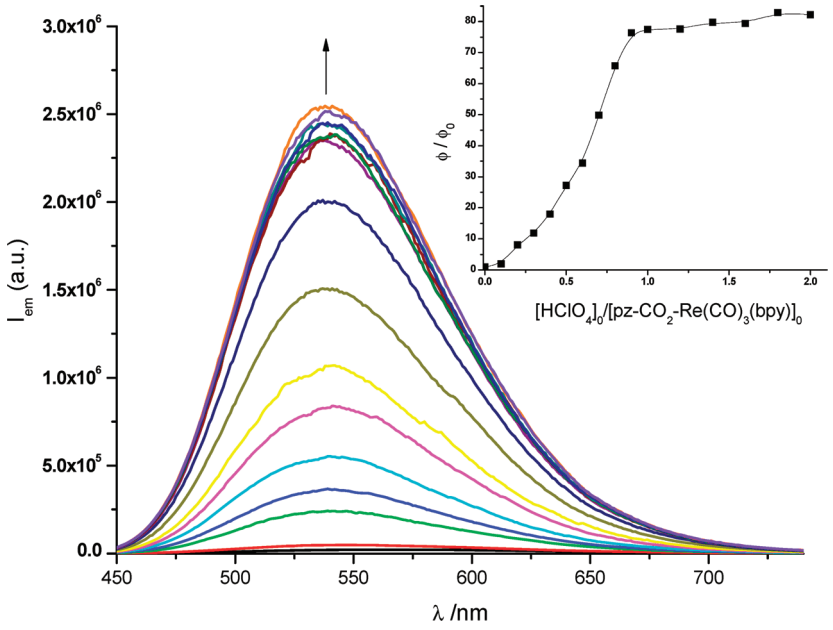

Figure 5. Luminescence spectra of the products after the termination of the reaction at different $[HClO_4]/[Re(I)]$ initial ratios (0, 0.1, 0.2, 0.3, 0.4, 0.5, 0.6, 0.7, 0.8, 0.9, 1.0, 1.2, 1.4, 1.6, 1.8, and 2.0). The arrow shows the progress of the change. The inset to Figure 2 shows the relative increase in the luminescence quantum yield as a function of $[HClO_4]/[Re(I)]$ initial ratio. See text for details.

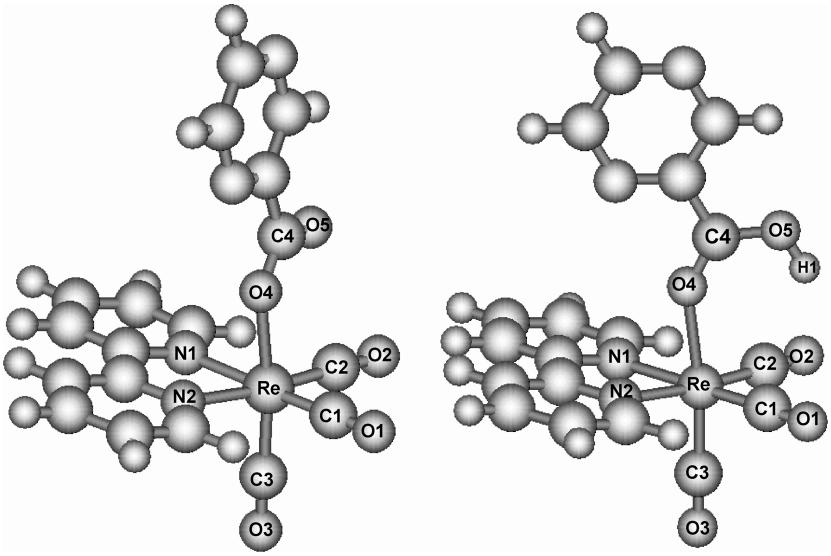

Figure 6. Molecular plot from DFT calculations of $pz-CO_2-Re(CO)_3(bpy)$ (left) and $[pz-C(OH)O-Re(CO)_3(bpy)]^+$ (right) showing the labeling of some relevant atoms that appear in Table 1.

observed at $t \sim 4$ min after the mixing of the reactants shows spectral features intermediate between those of $pz-CO_2-Re(CO)_3(bpy)$ and $Re(CO)_3(bpy)(CH_3CN)^+$ and could be attributed to the IR spectrum of the protonated intermediate, $[pz-C(OH)O-Re(CO)_3(bpy)]^+$, which was detected by UV–vis spectral changes at similar time delays after the initiation of the reaction. We also observed the appearance of the 1100 cm^{-1} band in $HClO_4-CH_3CN$ solutions, which is characteristic of free ClO_4^-.[44] This fact is indicating that, under our experimental conditions, $HClO_4$ is partially dissociated in acetonitrile solutions. Moreover, a small increase was observed in the absorbance at 1100 cm^{-1} during the course of the reaction which represented only an 8% increase in the concentration of free ClO_4^- relative to the initial concentration of ClO_4^- in $HClO_4-CH_3CN$ solutions.

The bands due to free pz–COOH, which usually appear around 1725 cm^{-1},[44,45] were observed between 1733 and 1753 cm^{-1} in the spectra of the reaction mixture (Figure 4a). Since the presence of a 1900 cm^{-1} band, characteristic of monomeric pz–COOH species,[46] was not observed in CH_3CN solutions containing pyrazinic acid, the existence of dimeric acid species could be inferred in that solvent.

The analysis of the IR spectral changes of Figure 4a, in the range between 1850 and 2100 cm^{-1}, was performed with chemometric

dx.doi.org/10.1021/jp206328q |J. Phys. Chem. A 2011, 115, 10979–10987

Table 1. Bond Distances (in Å) and Angles (in deg) around Rhenium in pz−CO_2−$Re(CO)_3$(bpy) and $[pz-C(OH)O-Re(CO)_3(bpy)]^+$ and around Carboxyl Group in pz−COOH

coordinate	pz−CO_2-$Re(CO)_3$(bpy)	pz−CO_2-$Re(CO)_3$(bpy)	$[pz-C(OH)O-Re(CO)_3(bpy)]^+$	pz−COOH
	X-ray	B98/LanL2DZ	B98/LanL2DZ	B98/LanL2DZ
		Bond Distances/Å		
Re−C1	1.883	1.918	1.926	
Re−C2	1.909	1.923	1.926	
Re−C3	1.904	1.906	1.900	
Re−O4	2.205	2.142	2.196	
Re−N1	2.164	2.166	2.161	
Re−N2	2.162	2.166	2.161	
C1−O1	1.195	1.190	1.186	
C2−O2	1.148	1.188	1.186	
C3−O3	1.117	1.192	1.186	
O4−C4	1.238	1.312	1.253	1.239
C4−O5	1.208	1.268	1.349	1.376
O5−H1	–	–	0.9823	0.9822
		Bond Angles / deg		
C1−Re−C2	87.7	89.2	89.2	
C1−Re−C3	87.8	90.6	89.5	
C2−Re−C3	89.5	89.9	89.4	
C1−Re−N1	175.1	172.2	172.7	
C2−Re−N1	96.9	97.2	96.9	
C3−Re−N1	93.7	94.0	93.5	
C1−Re−N2	99.9	97.5	97.0	
C2−Re−N2	172.0	172.5	172.6	
C3−Re−N2	93.0	93.4	93.7	
C1−Re−O4	94.9	92.4	95.9	
C2−Re−O4	95.9	96.8	96.3	
C3−Re−O4	174.0	172.7	172.2	
N1−Re−O4	83.1	82.4	80.1	
N2−Re−O4	81.3	79.6	80.5	
N1−Re−N2	75.5	75.9	76.2	
Re−O4−C4	121.2	128.8	144.4	
O4−C4−O5	127.1	125.7	124.1	123.0
C4−O5−H1	–	–	115.5	112.4

techniques. The number of independent contributions yielded $n = 3$. The spectral shapes obtained for the three species, i.e., pz−CO_2−$Re(CO)_3$(bpy), the protonated intermediate $[pz-C(OH)O-Re(CO)_3(bpy)]^+$, and the reaction product $Re(CO)_3(bpy)(CH_3CN)^+$, contributing to the spectral changes shown in Figure 4a are shown in Figure 4b. Figure 4c shows the calculated concentration profiles for the three species. It can be observed that at $t = 4$ min after the mixing of the reactants, the concentration of pz−CO_2−$Re(CO)_3$(bpy) has fallen to 12% of the initial concentration, 82% of the Re(I) complexes are protonated forming an intermediate, and 6% of the reactants have converted to products. This predominance of the protonated intermediate over the reactant was manifested also in the UV−vis spectra of Figure 1 at $t = 1$ min, which has spectral features of the protonated intermediate rather than of pz−CO_2−$Re(CO)_3$(bpy).

The amount of product formed after the termination of the reaction at different $[HClO_4]/[Re(I)]$ initial ratios was followed also by spectrofluorometric techniques. After the termination of the reaction, a large increase in the luminescence of the solution was observed (Figure 5). This is due to the higher luminescence quantum yield of $Re(CO)_3(bpy)(CH_3CN)^+$ than that of pz−CO_2−$Re(CO)_3$(bpy). In fact, the luminescence quantum yields were determined to be 0.52 and 0.007 for $Re(CO)_3(bpy)(CH_3CN)^+$ and pz−CO_2−$Re(CO)_3$(bpy), respectively. A $\phi_{em} = 0.52$ for $Re(CO)_3(bpy)(CH_3CN)^+$ in CH_3CN can be compared to $\phi_{em} = 0.41$ reported in the literature for the same complex in CH_2Cl_2.[43] The low ϕ_{em} of pz−CO_2−$Re(CO)_3$(bpy) is in accordance with similar low values of ϕ_{em} for other R−CO_2−$Re(CO)_3$(bpy) complexes.[20] The inset to Figure 5 shows that more than a 80-fold increase in the total luminescence of the solution is observed after the reaction between $HClO_4$ and pz−CO_2−$Re(CO)_3$(bpy). This increase in the total luminescence is in accordance to the relative luminescence quantum yields of $Re(CO)_3(bpy)(CH_3CN)^+$ and pz−CO_2−$Re(CO)_3$(bpy), which is $\phi_{product}/\phi_{reactant} = (0.52/0.007) \sim 75$.

Structural Characterization. The fully optimized CPCM-B98/LanL2DZ structures for pz−CO_2−$Re(CO)_3$(bpy) and $[pz-C(OH)O-Re(CO)_3(bpy)]^+$ are shown in Figure 6.

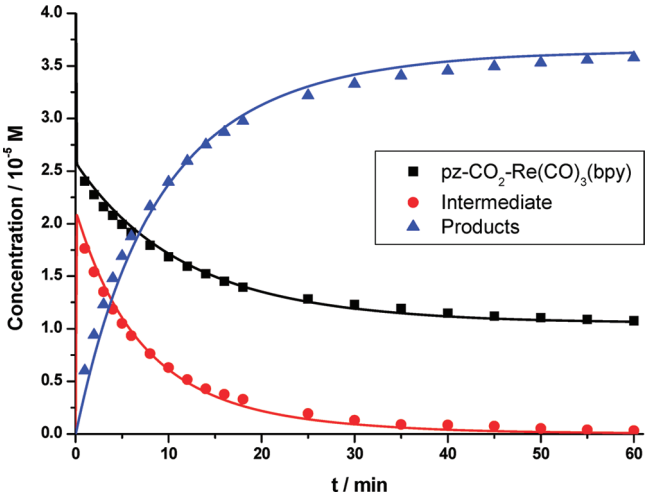

Figure 7. Comparison between concentration profiles obtained by MCR−ALS analysis (dots) and by numerical simulation using the Runge−Kutta method (lines). Initial concentrations: $[Re(I)] = 5 \times 10^{-5}$ M and $[HClO_4] = 4 \times 10^{-5}$ M. See text for details.

The derived bond lengths and bond angles for pz−CO_2−Re(CO)$_3$(bpy), [pz−C(OH)O−Re(CO)$_3$(bpy)]$^+$, and pz−COOH along with X-ray structure of pz−CO_2−Re(CO)$_3$(bpy)[16] are listed in Table 1. It can be observed that the experimental and calculated structural parameters of pz−CO_2−Re(CO)$_3$(bpy) are in good agreement. However, significant differences arise in the O4−C4 (calcd 1.312 Å, X-ray 1.238 Å), C4−O5 (calcd 1.268 Å, X-ray 1.208 Å), and Re−O4 (calcd 2.142 Å, X-ray 2.205 Å) distances and in the Re−O4−C4 (calcd 128.8°, X-ray 121.2°) angle. We note here that different rotations of the pyrazine group, relative to the bpy ligand, may generate almost isoenergetic stable configurations (with energy differences between rotamers within the value of kT, as was previously observed in DFT studies on similar Re(I) complexes[47]). These motions could contribute to the calculated geometry of pz−CO_2−Re(CO)$_3$(bpy) explaining the mentioned differences between X-ray and calculated geometries.

We turn now to compare the calculated geometry of [pz−C(OH)O−Re(CO)$_3$(bpy)]$^+$ to that of pz−CO_2−Re(CO)$_3$(bpy) . The protonated intermediate and the parent complex differ mainly by the relative orientation of the pyrazine ligand with respect to what we shall call the main plane of the molecule. This plane goes along the Re−CO_2 bond which links the pyrazine ligand to the Re and bisects the N−N bond of bpy. The pyrazine ligand is basically rotated by 70° between [pz−C(OH)O−Re(CO)$_3$(bpy)]$^+$ and pz−CO_2−Re(CO)$_3$(bpy) structures (see Figure 6). The comparison of bond distances and angles between the parent complex and the protonated intermediate shows that protonation of pz−CO_2−Re(CO)$_3$(bpy) at the O atom of the carboxylate bridge induces a lengthening of the Re−O4 and C4−O5 distances, a shortening of the C4−O4 distance, and an opening in the Re−O4−C4 angle (from 129° to 144°). Moreover, the protonated intermediate distances (C4−O5 and C4−O4) and the O4−C4−O5 angle are intermediate between those of pz−CO_2−Re(CO)$_3$(bpy) and pz−COOH.

Mechanistic Considerations. From conductometry measurements of diluted (5×10^{-5} M to 1×10^{-2} M) $HClO_4$ in CH_3CN, Kolthoff concluded that $HClO_4$ behaves as a strong acid in acetonitrile, thus dissociating completely the OH proton.[48] Later, however, from IR studies on more concentrated solutions, it was considered that the formation of an H-bonding adduct between CH_3CN and $HClO_4$, i.e., [$CH_3CNHClO_4$] in ref 44, occurred in the initial stage of the interaction between the acid and the nonprotic solvent and the dissociation of the OH proton did not occur at ∼0.2 M concentrations in CH_3CN.[44] Nevertheless, pK_a values of $HClO_4$ in CH_3CN, as determined conductometrically, range from 1.6[49] to 2.1.[50,51] In a more recent report, however, the acidity of $HClO_4$ was directly measured relative to picric acid in 1,2-dichloroethane as a solvent, and a pK_a of −0.7[52] was calculated for that acid in CH_3CN. Moreover, at a concentration of 0.026 M in CH_3CN (though in the presence of $[H_2O] = 0.1$ M), the acid was determined to be dissociated at 88%.[53] Additionally, it is important to note that our IR measurements have shown the presence of free ClO_4^- in diluted acetonitrile solutions of perchloric acid as well as a very small increase in its concentration during the kinetic runs. Therefore, under our experimental conditions, i.e., 5×10^{-6} M ≤ $[HClO_4] \leq 1 \times 10^{-4}$ M, the equilibrium of eq 4 should be displaced to the right:

$$CH_3CN + HClO_4 \rightleftarrows [CH_3CNHClO_4] \rightleftarrows H^+(solv) + ClO_4^-(solv) \quad (4)$$

In the case of perchloric acid, hydrogen ions that appear in the solution are known to form hydrates $H_3O^+ \cdot nH_2O$ with adventitious water molecules[53,54] (a minimum $[H_2O] = 2 \times 10^{-3}$ M can be expected in our experiments from the water content of CH_3CN). Even in solvents which are very weak bases, like CH_3CN, hydrogen bonding between an anion and its conjugate acid is likely to occur, giving rise to dimers.[55] Therefore, H^+(solv) and ClO_4^-(solv) in eq 4 are probably not the real chemical species existing in CH_3CN solutions.

The concentration profiles obtained by MCR−ALS analysis of time-resolved matrices of either UV−vis or IR spectra suggest the following mechanism, eqs 5−7:

$$pz - CO_2 - Re(CO)_3(bpy) + H^+ \rightleftarrows [pz - C(OH)O - Re(CO)_3(bpy)]^+ \quad (5)$$

$$[pz - C(OH)O - Re(CO)_3(bpy)]^+ \rightarrow pz - COOH + [Re(CO)_3(bpy)]^+ \quad (6)$$

$$[Re(CO)_3(bpy)]^+ + CH_3CN \rightarrow Re(CO)_3(bpy)(CH_3CN)^+ \quad (7)$$

The intermediate formed by reaction 6 ([Re(CO)$_3$(bpy)]$^+$) can be a pentacoordinate complex resulting from the elimination of pz−COOH from the protonated intermediate [pz−C(OH)O−Re(CO)$_3$(bpy)]$^+$. This pentacoordinate complex should very rapidly react with a solvent molecule to yield the final product, Re(CO)$_3$(bpy)(CH_3CN)$^+$. The overall rate constant of eqs 6−7 should be of first order in the protonated intermediate since the solvation of [Re(CO)$_3$(bpy)]$^+$ is likely to be much faster than the decomposition of [pz−C(OH)O−Re(CO)$_3$(bpy)]$^+$.

Assuming that eq 6 is the rate-determining step, the mathematical description of the kinetic system involves the solution of three coupled differential equations. Therefore, the proposed mechanism was numerically simulated by using the Runge−Kutta method of fourth order. Model parameters were estimated by nonlinear regression fitting of the concentration profiles obtained by MCR−ALS analysis, yielding values of log(K_5) = 4.9 ± 0.3 and

$k_6 = 0.16 \pm 0.03\ \mathrm{min}^{-1}$ for the formation equilibrium constant and the decay rate constant of the protonated intermediate, respectively.

Figure 7 shows that there is a reasonably good agreement between the experimental and the calculated concentration profiles for pz−CO_2−Re(CO)$_3$(bpy), [pz−C(OH)O−Re(CO)$_3$(bpy)]$^+$, and the sum of the two products (Re(CO)$_3$(bpy)(CH$_3$CN)$^+$ and pz−COOH). The large equilibrium constant explains the predominance of the protonated intermediate over the reactant at short times observed in UV−vis and IR spectroscopies.

It is noteworthy that, in addition to the set of eqs 5−7, other reactions such as eqs 8−9 may play a role in the behavior of the system:

$$CH_3CN + pz{-}COOH \rightleftarrows [CH_3CN\ HO{-}C(O) - pz] \quad (8)$$

$$[CH_3CNHO{-}C(O){-}pz] + H^+ \rightleftarrows [pz{-}COOH_2]^+ + CH_3CN \quad (9)$$

Similar equilibriums like those of eqs 8−9 have been observed in IR studies of the interaction between $HClO_4$ and CH_3CO_2H acids in acetonitrile.[44] When the concentration of pz−COOH becomes comparable to that of pz−CO_2−Re(CO)$_3$(bpy) in the solution, the equilibrium process of eq 9 may be in competition with the protonation reaction of the Re(I) complex.

CONCLUSIONS

The protonation of the complex pz−CO_2−Re(CO)$_3$(bpy) by $HClO_4$ in CH_3CN yields pz−COOH and Re(CO)$_3$(bpy)(CH$_3$CN)$^+$ as the main reaction products via the protonated intermediate [pz−C(OH)O−Re(CO)$_3$(bpy)]$^+$. A fast equilibrium is established between solvated protons, pz−CO_2−Re(CO)$_3$(bpy), and [pz−C(OH)O−Re(CO)$_3$(bpy)]$^+$. This intermediate has been characterized by UV−vis and IR spectroscopies and by DFT calculations. Moreover, the protonated intermediate distances (C4−O5 and C4−O4) and O4−C4−O5 angle are intermediate between those of pz−CO_2−Re(CO)$_3$(bpy) and pz−COOH. The kinetics of the protonation reaction was studied by following the UV−vis and IR spectral changes in different reaction conditions. The MCR−ALS method was employed to calculate the concentration profiles from the full matrix of time-resolved UV−vis spectra. The proposed mechanism was numerically simulated by using Runge−Kutta methods. Model parameters were estimated by nonlinear regression fitting of the concentration profiles, yielding values of $\log(K_S) = 4.9 \pm 0.3$ and $k_6 = 0.16 \pm 0.03\ \mathrm{min}^{-1}$ for the formation equilibrium constant and the decay rate constant of the protonated intermediate, respectively. After the termination of the reaction, a large increase in the luminescence of the solution was observed due to the higher luminescence quantum yield of Re(CO)$_3$(bpy)(CH$_3$CN)$^+$ compared to that of pz−CO_2−Re(CO)$_3$(bpy). The latter observation suggests the possibility that the protonolysis of the Re−carboxylate bond in pz−CO_2−Re(CO)$_3$(bpy) could be utilized for the development of a device capable of detecting proton traces in aprotic media as well as in a pH-sensing material.

AUTHOR INFORMATION

Corresponding Author

*E-mail: ewolcan@inifta.unlp.edu.ar.

ACKNOWLEDGMENT

This work was supported in part by ANPCyT Grant No. PICT 26195, CONICET-PIP 0389, Universidad Nacional de La Plata, and CICPBA. FTIR measurements were performed at Dr. Adela Croce's laboratory. We thank Dr. A.C. for hosting our visits to her laboratory. U.N.F. acknowledges support from CONICET. C.J.C, F.S.G.E, G.T.R., and E.W. are members of CONICET, and M.R.F. is a member of CICPBA.

REFERENCES

(1) Vlček, A. Ultrafast Excited-State Processes in Re(I) Carbonyl−Diimine Complexes: From Excitation to Photochemistry. In *Photophysics of Organometallics*; Lees, A. J., Ed.; Springer: Berlin/Heidelberg, Germany, 2010; Vol. 29, pp 73−114.

(2) Kirgan, R.; Sullivan, B.; Rillema, D. *Photochemistry and Photophysics of Coordination Compounds: Rhenium Photochemistry and Photophysics of Coordination Compounds II*; Balzani, V., Campagna, S., Eds.; Springer: Berlin/Heidelberg, Germany, 2007; Vol. 281, pp 45−100.

(3) Fox, M. A.; Chanon, M. *Photoinduced Electron Transfer*; Elsevier: Amsterdam, The Netherlands, 1988.

(4) Balzani, V.; Bolletta, F.; Gandolfi, M.; Maestri, M. Bimolecular Electron Transfer Reactions of the Excited States of Transition Metal Complexes. In *Organic Chemistry and Theory*; Springer: Berlin/Heidelberg, Germany, 1978; Vol. 75, pp 1−64.

(5) Grätzel, M. *Energy Resources Through Photochemistry and Catalysis,*; Academic Press: New York, 1983.

(6) Kalyanasundaram, K. *Coord. Chem. Rev.* **1982**, *46*, 159–244.

(7) Kalyanasundaram, K.; Grätzel, M. *Photosensitization and Photocatalysis Using Inorganic and Organometallic Compounds*; Kluwer Academic Publishers: Dordrecht, Germany, 1993.

(8) Gholamkhass, B.; Mametsuka, H.; Koike, K.; Tanabe, T.; Furue, M.; Ishitani, O. *Inorg. Chem.* **2005**, *44*, 2326–2336.

(9) Sacksteder, L.; Lee, M.; Demas, J. N.; DeGraff, B. A. *J. Am. Chem. Soc.* **1993**, *115*, 8230–8238.

(10) Yam, V. W.-W.; Wong, K. M.-C.; Lee, V. W.-M.; Lo, K. K.-W.; Cheung, K.-K. *Organometallics* **1995**, *14*, 4034–4036.

(11) Yoon, D. I.; Berg-Brennan, C. A.; Lu, H.; Hupp, J. T. *Inorg. Chem.* **1992**, *31*, 3192–3194.

(12) Calabrese, J. C.; Tam, W. *Chem. Phys. Lett.* **1987**, *133*, 244–245.

(13) Ehler, T. T.; Malmberg, N.; Carron, K.; Sullivan, B. P.; Noe, L. J. *J. Phys. Chem. B* **1997**, *101*, 3174–3180.

(14) Yam, V. W.-W.; Lau, V. C.-Y.; Cheung, K.-K. *J. Chem. Soc., Chem. Commun.* **1995**, 259–261.

(15) Higgins, B.; DeGraff, B. A.; Demas, J. N. *Inorg. Chem.* **2005**, *44*, 6662–6669.

(16) Guerrero, J.; Piro, O. E.; Wolcan, E.; Feliz, M. R.; Ferraudi, G.; Moya, S. A. *Organometallics* **2001**, *20*, 2842–2853.

(17) Juliarena, M. P.; Lezna, R. O.; Ruiz, G. T.; Féliz, M. R.; Ferraudi, G. J.; Wolcan, E. *Polyhedron* **2008**, *27*, 1471–1478.

(18) Juliarena, M. P.; Ruiz, G. T.; Wolcan, E.; Lezna, R. O.; Feliz, M. R.; Ferraudi, G.; Guerrero, J. *Organometallics* **2007**, *26*, 272–280.

(19) Ruiz, G. T.; Juliarena, M. P.; Lezna, R. O.; Wolcan, E.; Feliz, M. R.; Ferraudi, G. *Helv. Chim. Acta* **2002**, *85*, 1261–1275.

(20) Wolcan, E.; Torchia, G.; Tocho, J.; Piro, O. E.; Juliarena, P.; Ruiza, G.; Féliz, M. R. *J. Chem. Soc., Dalton Trans.* **2002**, 2194–2202.

(21) Wolcan, E.; Féliz, M. R. *Photochem. Photobiol. Sci.* **2003**, *2*, 412–417.

(22) García Einschlag, F. *Kinesim 9.5: Obra de software*; Dirección Nacional del Derecho de Autor, Argentina. Expediente No. 395814, 2005.

(23) Ruckebusch, C.; Aloise, S; Blanchet, L.; Huvenne, J. P.; Buntinx, G. *Chemom. Intell. Lab. Syst.* **2008**, *91*, 17–27.

(24) Tauler, R. *Chemom. Intell. Lab. Syst.* **1995**, *30*, 133–146.

(25) Garrido, M.; Larrechi, M. S.; Rius, F. X.; Tauler, R. *Chemom. Intell. Lab. Syst.* **2005**, *76*, 111–120.

(26) Garrido, M.; Lázaro, I.; Larrechi, M. S.; Rius, F. X. *Anal. Chim. Acta* **2004**, *515*, 65–73.

(27) Blanco, M.; Peinado, A. C.; Mas, J. *Anal. Chim. Acta* **2005**, *544*, 199–205.
(28) Meloun, M.; Čapek, J.; Mikšik, P.; Brereton, R. G. *Anal. Chim. Acta* **2000**, *423*, 51–68.
(29) de Juan, A.; Tauler, R. *Anal. Chim. Acta* **2003**, *500*, 195–210.
(30) Gemperline, P.; Cash, E. *Anal. Chem.* **2003**, *75*, 4236–4243.
(31) Puxty, G.; Maeder, M.; Hungerbühler, K. *Chemom. Intell. Lab. Syst.* **2006**, *81*, 149–164.
(32) Bevington, P. *Data Reduction Analysis*; McGraw-Hill: New York, 1969; Chapter 11, pp 208−222.
(33) Vlcek, A., Jr; Zális, S. *Coord. Chem. Rev.* **2007**, *251*, 258–287.
(34) Gao, Y.; Sun, S.; Han, K. *Spectrochim. Acta, Part A* **2009**, *71*, 2016–2022.
(35) Schmider, H. L.; Becke, A. D. *J. Chem. Phys.* **1998**, *108*, 9624–9631.
(36) Frisch, M. J.; Trucks, G. W.; Schlegel, H. B.; Scuseria, G. E.; Robb, M. A.; Cheeseman, J. R.; Scalmani, G.; Barone, V.; Mennucci, B.; Petersson, G. A.; Nakatsuji, H.; Caricato, M.; Li, X.; Hratchian, H. P.; Izmaylov, A. F.; Bloino, J.; Zheng, G.; Sonnenberg, J. L.; Hada, M.; Ehara, M.; Toyota, K.; Fukuda, R.; Hasegawa, J.; Ishida, M.; Nakajima, T.; Honda, Y.; Kitao, O.; Nakai, H.; Vreven, T.; Montgomery, J. A.; , Jr.; Peralta, J. E.; Ogliaro, F.; Bearpark, M.; Heyd, J. J.; Brothers, E.; Kudin, K. N.; Staroverov, V. N.; Kobayashi, R.; Normand, J.; Raghavachari, K.; Rendell, A.; Burant, J. C.; Iyengar, S. S.; Tomasi, J.; Cossi, M.; Rega, N.; Millam, J. M.; Klene, M.; Knox, J. E.; Cross, J. B.; Bakken, V.; Adamo, C.; Jaramillo, J.; Gomperts, R.; Stratmann, R. E.; Yazyev, O.; Austin, A. J.; Cammi, R.; Pomelli, C.; Ochterski, J. W.; Martin, R. L.; Morokuma, K.; Zakrzewski, V. G.; Voth, G. A.; Salvador, P.; Dannenberg, J. J.; Dapprich, S.; Daniels, A. D.; Farkas, O.; Foresman, J. B.; Ortiz, J. V.; Cioslowski, J.; Fox, D. J. *Gaussian 09*, revision A.02; Gaussian, Inc.: Wallingford CT, 2009.
(37) Frisch, M. J.; Pople, J. A.; Binkley, J. S. *J. Chem. Phys.* **1984**, *80*, 3265–3269 and references therein.
(38) Woon, D. E.; Dunning, J. T. H. *J. Chem. Phys.* **1993**, *98*, 1358–1371 and references therein.
(39) Hay, P. J.; Wadt, W. R. *J. Chem. Phys.* **1985**, *82*, 270–283.
(40) Barone, V.; Cossi, M. *J. Phys. Chem. A* **1998**, *102*, 1995–2001.
(41) Garrido Frenich, A.; Picón Zamora, D.; Martínez Vidal, J. L.; Martínez Galera, M. *Anal. Chim. Acta* **2001**, *449*, 143–155.
(42) Werrett, M. V.; Chartrand, D.; Gale, J. D.; Hanan, G. S.; MacLellan, J. G.; Massi, M.; Muzzioli, S.; Raiteri, P.; Skelton, B. W.; Silberstein, M.; Stagni, S. *Inorg. Chem.* **2011**, *50*, 1229–1241.
(43) Caspar, J. V.; Meyer, T. J. *J. Phys. Chem.* **1983**, *87*, 952–957.
(44) Kinugasa, M.; Kishi, K.; Ikeda, S. *J. Phys. Chem.* **1973**, *77*, 1914–1918.
(45) Goher, M. A. S.; Mak, T. C. W. *Polyhedron* **1995**, *14*, 2587–2594.
(46) De Sa, G. F.; De B. Neto, B.; Ferreira, R. *Inorg. Chim. Acta* **1977**, *23*, 249–252.
(47) Kayanuma, M.; Daniel, C.; Köppel, H.; Gindensperger, E. *Coord. Chem. Rev.* **2011**in press.
(48) Coetzee, J. F.; Kolthoff, I. M. *J. Am. Chem. Soc.* **1957**, *79*, 6110–6115.
(49) Fujinaga, T.; Sakamoto, I. *J. Electroanal. Chem.* **1977**, *85*, 185–201.
(50) Coetzee, J. F.; McGuire, D. K. *J. Phys. Chem.* **1963**, *67*, 1810–1814.
(51) Coetzee, J. F. *Prog. Phys. Org. Chem.* **1967**, *4*, 45–92.
(52) Kütt, A.; Rodima, T.; Saame, J.; Raamat, E.; Mäemets, V.; Kaljurand, I.; Koppel, I. A.; Garlyauskayte, R. Y.; Yagupolskii, Y. L.; Yagupolskii, L. M.; Bernhardt, E.; Willner, H.; Leito, I. *J. Org. Chem.* **2010**, *76*, 391–395.
(53) Troshin, V.; Sheludyakova, L.; Mironov, I. *J. Anal. Chem.* **2008**, *63*, 544–547.
(54) Kolthoff, I. M.; Chantooni, M. K. *J. Am. Chem. Soc.* **1968**, *90*, 3320–3326.
(55) Kolthoff, I. M. *Anal. Chem.* **1974**, *46*, 1992–2003.